# Renewable Chemical Commodity Feedstocks from Integrated Catalytic Processing of Pyrolysis Oils

Tushar P. Vispute, *et al.*

*Science* **330**, 1222 (2010);
DOI: 10.1126/science.1194218

adequate for the industrially relevant synthesis of cumene through the alkylation of benzene with propylene because it should give lower yields of undesired secondary products when compared with the commercially used 12-ring beta zeolite. We have checked this possibility and analyzed the results of selectivity versus conversion for cumene/propylene alkylation on Al-ITQ-47 and beta (fig. S10). Regardless of the level of conversion considered, the selectivity to cumene is always greater for Al-ITQ-47 with boggsite structure than for beta zeolite. However, the activity of beta zeolite is greater than Al-ITQ-47 because of the smaller crystal size of beta zeolite than that of boggsite (fig. S11).

### References and Notes


1. J. Jiang, J. Yu, A. Corma, *Angew. Chem. Int. Ed.* **49**, 3120 (2010).
2. A. W. Burton, S. I. Zones, S. Elomari, *Curr. Opin. Colloid Interface Sci.* **10**, 211 (2005).
3. J. Sun *et al.*, *Nature* **458**, 1154 (2009).
4. R. F. Lobo, S. I. Zones, M. E. Davis, *J. Inclusion Phenom. Mol. Recognit. Chem.* **21**, 47 (1995).
5. A. Jackowski, S. I. Zones, S.-J. Hwang, A. W. Burton, *J. Am. Chem. Soc.* **131**, 1092 (2009).
6. R. H. Archer, S. I. Zones, M. E. Davis, *Microporous Mesoporous Mater.* **130**, 255 (2010).
7. D. L. Dorset *et al.*, *J. Am. Chem. Soc.* **128**, 8862 (2006).
8. A. Corma *et al.*, *J. Am. Chem. Soc.* **130**, 16482 (2008).
9. D. L. Dorset *et al.*, *Chem. Mater.* **20**, 5325 (2008).
10. A. Corma *et al.*, *Proc. Natl. Acad. Sci. U.S.A.* **107**, 11935 (2010).
11. A. Corma, *Microporous Mesoporous Mater.* **21**, 487 (1998).
12. M. D. Shannon, J. L. Casci, P. A. Cox, S. J. Andrews, *Nature* **353**, 417 (1995).
13. R. F. Lobo *et al.*, *Science* **3**, 1543 (1993).
14. S. I. Zones, M. M. Olmsted, D. S. Santilli, *J. Am. Chem. Soc.* **114**, 4195 (1992).
15. S. I. Zones *et al.*, U.S. Patent 491006 (1990).
16. R. F. Lobo, M. E. Davis, *J. Am. Chem. Soc.* **117**, 3766 (1995).
17. R. Castañeda, A. Corma, V. Fornés, F. Rey, J. Rius, *J. Am. Chem. Soc.* **125**, 7820 (2003).
18. J. J. Pluth, J. S. Smith, *Am. Mineral.* **75**, 501 (1990).
19. E. Galli, S. Quartieri, G. Vezzalini, A. Alberti, *Eur. J. Mineral.* **7**, 1029 (1995).
20. Ch. Baerlocher, L. B. McCusker, D. H. Olson, *Atlas of Zeolite Framework Types* (Elsevier, Amsterdam, ed. 6, 2007).
21. A. Corma, F. Rey, S. Valencia, J. L. Jordá, J. Rius, *Nat. Mater.* **2**, 493 (2003).
22. D. L. Dorset, S. C. Weston, S. S. Dhingra, *J. Phys. Chem. B* **110**, 2045 (2006).
23. S. Elomari, A. Burtin, R. C. Medrud, R. Grosse-Kunstleve, *Microporous Mesoporous Mater.* **118**, 325 (2009).
24. L. Josien, A. Simon-Masseron, V. Gramlich, J. Patarin, L. Rouleau, *Chemistry* **9**, 856 (2003).
25. Materials and methods are available as supporting material on *Science* Online.
26. R. Schwesinger *et al.*, *Liebigs Ann.* **7**, 1055 (1996).
27. D. G. Howard, R. W. Tschernich, J. V. Smith, G. L. Klein, *Am. Mineral.* **75**, 1200 (1990).
28. C. Fild, D. F. Shantz, R. F. Lobo, H. Koller, *Phys. Chem. Chem. Phys.* **2**, 3091 (2000).
29. R. H. Koller, C. Fild, R. F. Lobo, *Microporous Mesoporous Mater.* **79**, 215 (2005).
30. C. Chen, S. I. Zones, *Stud. Surf. Sci. Catal.* **135**, 1710 (2001).


31. The authors thank the Spanish government (projects MAT2009-14528-C02-01, PLE2009-0054, and CONSOLIDER INGENIO 2010) and Generalitat Valenciana (Project Prometeo) for financial support. R.S. and N.V. thank UPV and CSIC for Programa de Formacion de Personal Investigador and Junta para la Ampliación de Estudios predoctoral fellowships, respectively. Further details on the crystal structure may be obtained from the Fachinformationszentrum Karlsruhe, D-76344 Eggenstein-Leopoldshafen, Germany [fax: (+49) 7247-808-666; e-mail: crysdata@fiz-Karlruhe.de], on quoting the depository number CDS-422193.


### Supporting Online Material

www.sciencemag.org/cgi/content/full/330/6008/1219/DC1
Materials and Methods
Figs. S1 to S11
Tables S1 to S4
References

9 August 2010; accepted 14 October 2010
10.1126/science.1196240

# Renewable Chemical Commodity Feedstocks from Integrated Catalytic Processing of Pyrolysis Oils

**Tushar P. Vispute,[1] Huiyan Zhang,[1,2] Aimaro Sanna,[1,3] Rui Xiao,[2] George W. Huber[1]**

**Fast pyrolysis of lignocellulosic biomass produces a renewable liquid fuel called pyrolysis oil that is the cheapest liquid fuel produced from biomass today. Here we show that pyrolysis oils can be converted into industrial commodity chemical feedstocks using an integrated catalytic approach that combines hydroprocessing with zeolite catalysis. The hydroprocessing increases the intrinsic hydrogen content of the pyrolysis oil, producing polyols and alcohols. The zeolite catalyst then converts these hydrogenated products into light olefins and aromatic hydrocarbons in a yield as much as three times higher than that produced with the pure pyrolysis oil. The yield of aromatic hydrocarbons and light olefins from the biomass conversion over zeolite is proportional to the intrinsic amount of hydrogen added to the biomass feedstock during hydroprocessing. The total product yield can be adjusted depending on market values of the chemical feedstocks and the relative prices of the hydrogen and biomass.**

Dwindling petroleum resources combined with economic, environmental, and political concerns about the petroleum-based economy make it imperative to develop new processes for the production of renewable fuels and chemicals (*1*–*3*). Lignocellulosic biomass is the most abundant and inexpensive sustainable source of carbon that can be used as a feedstock for the production of renewable fuels and commodity chemical feedstocks (*4*). Pyrolysis oils or bio-oils have been identified as inexpensive renewable liquid fuel that can be produced from lignocellulosic biomass (*5*–*7*). Fast pyrolysis of biomass has been shown to be two to three times cheaper than biomass conversion technologies based on gasification and fermentation processes (*8*). However, bio-oils are low-quality fuels that cannot be used in conventional gasoline and diesel fuel engines because they are immiscible with petroleum-derived fuels, primarily on account of their high oxygen content [up to 60 weight % (wt %)] (*5*, *7*, *9*). Other challenges with pyrolysis oils are that they are acidic, have a high water content (25 to 50 wt %), and constitute an emulsion that will phase-separate when stored. Ideally, pyrolysis oils should be deoxygenated to a mixture of organic molecules that are more compatible with current fuels and chemical manufacturing infrastructure (*10*). Several approaches toward this end are currently being studied, including hydrotreating of bio-oils (*10*, *11*), zeolite conversion of bio-oils (*12*, *13*), and aqueous-phase processing of bio-oils (*14*). However, none of these approaches are used commercially today, primarily because they produce low yields of fungible products.

In this paper, we outline a distinct strategy for bio-oil deoxygenation into high-yield commodity chemicals, including C2 to C6 monohydric alcohols and diols, C6 to C8 aromatic hydrocarbons, and C2 to C4 olefins with over 60% overall carbon yields. Our approach involves hydroprocessing of the bio-oils over supported metal catalysts, followed by conversion over zeolite catalysts. It is not possible to completely hydrodeoxygenate the pyrolysis oil in a packed-bed reactor without frequent catalyst regeneration because of coke formation on the catalyst surface. Furthermore, complete hydrodeoxygenation requires large amounts of expensive hydrogen. In our process, drawbacks associated with the prior bio-oil hydrogenation processes are overcome by operating at moderate temperatures (≤250°C) at which no catalyst coking or reactor plugging was observed. Furthermore, our process can produce products without the high hydrogen requirements. Employing a zeolite upgrading step at the end has the advantage that a fluidized bed reactor can be used, where the coked catalyst can be regenerated by burning off the coke and recy-

[1]Department of Chemical Engineering, University of Massachusetts–Amherst, Amherst, MA 01003, USA. [2]School of Energy and Environment, Southeast University, Nanjing 210096, People's Republic of China. [3]Energy and Sustainability Research Division, Department of Chemical and Environmental Engineering, University of Nottingham, University Park, Nottingham, NG7 2RD, UK.

cled back to the reactor. The goal of this report is to demonstrate how pyrolysis oil could practically be upgraded through catalytic processes into commodity chemicals.

The integrated catalytic approach presented in this report can be tuned to produce different targeted distributions of organic small molecules that fit seamlessly into the existing petrochemical infrastructure. The products can be tuned to change with different market conditions. The C6 to C8 aromatic hydrocarbons can be high-octane gasoline additives or feedstocks for the chemical and polymer industries (*15*). The C2 to C4 olefins can also be used directly for polymer synthesis or can be modified to form other products, including alkylated aromatics (*16*, *17*) and longer linear alpha olefins (*18*). The gasoline-range alcohols can be high-octane gasoline additives. The C2 to C6 diols can serve as feedstocks for the chemical and polymer industries. The chemical industry relies on seven primary building blocks that are all derived from petroleum-based processes: benzene, toluene, xylene, ethylene, propylene, 1,3-butadiene, and methanol (*19*). Our catalytic process produces five of these seven petrochemical feedstocks, which opens the door to a chemical industry based on renewable biomass feedstock.

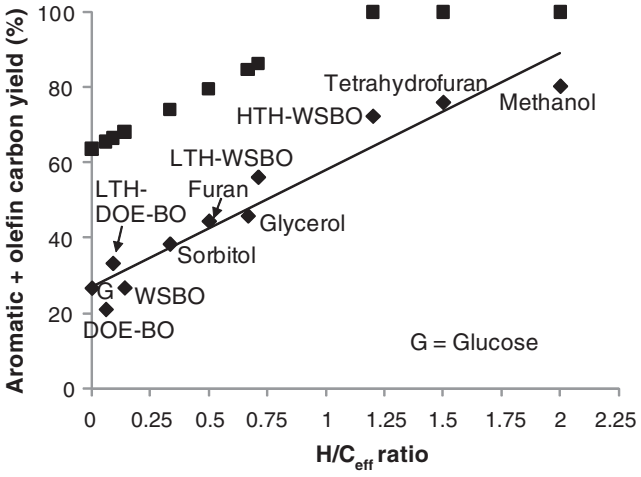


**Fig. 1.** Carbon yield of olefins and aromatic hydrocarbons from the conversion of biomass-derived feedstocks over a HZSM-5 catalyst as a function of the H/C$_{eff}$ ratio of the feed. Diamonds, experimental yield; squares, theoretical yield. The theoretical yield is calculated for toluene (see table S8 and accompanying text). WSBO, water-soluble fraction of the pinewood bio-oil; LTH-WSBO, WSBO hydrogenated over Ru/C [at 398 K and 52 bar at weight hourly space velocity (WHSV) of 3 hour$^{-1}$]; HTH-WSBO, WSBO hydrogenated first over Ru/C (at 398 K and 100 bar at WHSV of 3 hour$^{-1}$), then over Pt/C (at 523 K and 100 bar at WHSV of 3 hour$^{-1}$); DOE-BO, DOE bio-oil; LTH-DOE-BO, DOE-BO hydrogenated over Ru/C (at 398 K and 100 bar at WHSV of 1.6 hour$^{-1}$).

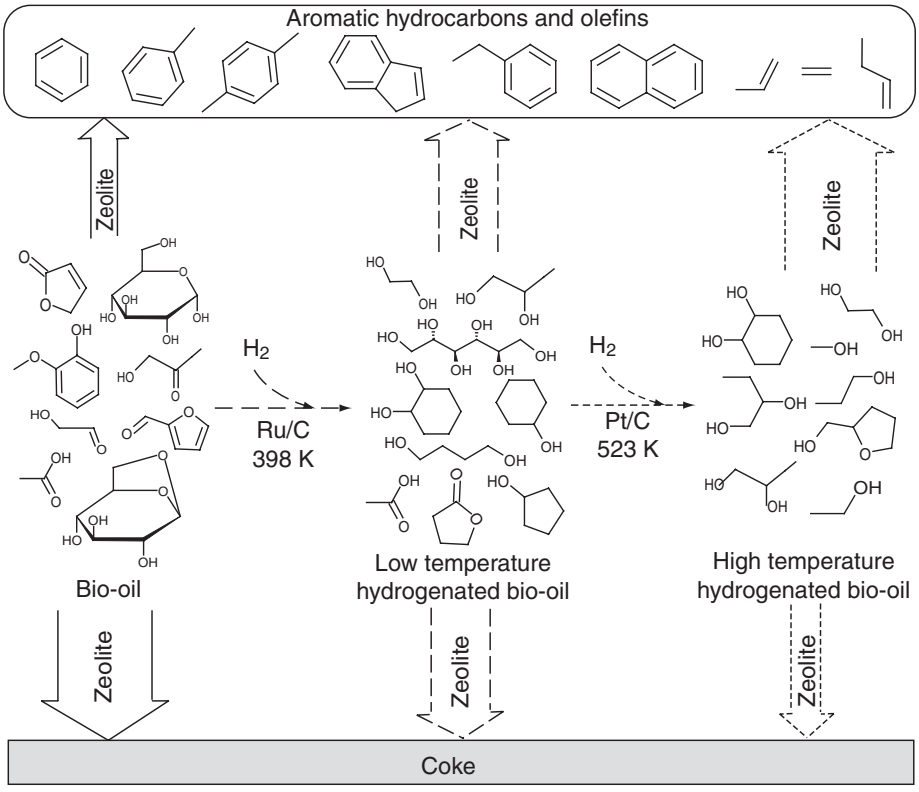


**Fig. 2.** Reaction schematic for the integrated hydroprocessing and zeolite upgrading of pyrolysis oil. Solid arrows: Pyrolysis oil is directly passed over the zeolite catalyst; long-dashed arrows: Pyrolysis oil is hydrogenated over Ru/C at 398 K and then passed over the zeolite catalyst; short-dashed arrows: Pyrolysis oil is first hydrogenated over Ru/C at 398 K, then over Pt/C at 523 K, and then passed over the zeolite catalyst. The width of the vertical arrows represents the product carbon yield from a particular field. In addition to the product streams shown in the figure, oxygen is removed at the zeolite stage as a mixture of CO, $CO_2$, and $H_2O$. Boosting the hydrogen content of the zeolite feed (left to right) increases the thermal stability of the feed, resulting in a reduction in amount of coke and an increase in the yields of aromatic hydrocarbons and olefins. The addition of hydrogen also raises the proportion of oxygen lost as water relative to CO and $CO_2$ and thereby further raises the proportion of carbon incorporated into marketable compounds.

The hydrogen content of a particular feedstock can be expressed in terms of its hydrogen-to-carbon atomic effective ratio (H/C$_{eff}$ ratio), as defined in Eq. 1. The H/C$_{eff}$ ratio is equal to the number of atoms of hydrogen minus twice the number of atoms of oxygen divided by the number of atoms of carbon in a feedstock. Lignocellulosic biomass and carbohydrate-based feedstocks have H/C$_{eff}$ ratios between 0 and 0.5. In contrast, petroleum-based feedstocks have H/C$_{eff}$ ratios from 1.0 to 2.0. Thus, biomass-based feedstocks are hydrogen-deficient because of the presence of oxygen. For example, the bio-oil used in this study has an H/C$_{eff}$ ratio of 0.06. During the conversion of biomass to deoxygenated compounds, the oxygen can be removed as a combination of CO, $CO_2$, and $H_2O$. Adding external hydrogen to supplement the hydrogen in the biomass itself boosts the proportion of oxygen removed as $H_2O$ versus CO and $CO_2$. The exact ratios of CO, $CO_2$, and $H_2O$ can be determined from the reaction stoichiometry between the feeds and the products. Thus, the addition of external hydrogen can increase the carbon yield of commodity chemicals produced from pyrolysis oils. This relation demonstrates how the biomass-refining industry could be tied to the hydrogen economy.

$$\mathrm{H/C_{eff}} = \frac{\text{moles of H} - (2 \times \text{moles of O})}{\text{moles of C}} \quad (1)$$

In this study, we converted 11 different biomass-derived feedstocks, with a range of different functionalities over a ZSM-5 catalyst. This catalyst has the proper pore structure and active sites to effectively convert biomass-derived molecules into aromatic hydrocarbons and olefins (*20*–*22*). Figure 1 shows that the aromatic and olefin yield increases with the H/C$_{eff}$ ratio of the feedstock (details in table S5), and this relationship is applicable to a wide variety of biomass-derived feedstocks. The theoretical yield (table S8 and accompanying text), also shown

in Fig. 1, increases with the $H/C_{eff}$ ratio as well. The increase in the aromatic and olefin yield with increasing $H/C_{eff}$ ratio is due to two different phenomena: an increase in the thermal stability of the feedstock and an increase in the intrinsic amount of hydrogen in the feedstock. Increasing the $H/C_{eff}$ ratio improves the thermal stability of the biomass-derived molecules by hydrogenating the functionalities (primarily aldehydes and ketones) that otherwise thermally decompose to char as shown in table S7. For example, in thermogravimetric studies, glucose produces 23.1 wt % coke when heated to 973 K under a helium atmosphere (table S7). Sorbitol, a glucose derivative in which the aldehyde functionality has been hydrogenated to an alcohol, is substantially more thermally stable and produces only 6.1 wt % coke. Increasing the $H/C_{eff}$ ratio also increases the intrinsic hydrogen content of the biomass-derived feedstock, which allows a higher theoretical yield of aromatic hydrocarbons and olefins from these feedstocks, because less carbon is used for the deoxygenation (table S8).

In this same respect, bio-oil and its aqueous fraction can be stabilized by hydroprocessing, and at the same time an increase in intrinsic hydrogen content results in higher aromatic and olefin yields. Figure 2 shows a generic reaction scheme for the conversion of bio-oil (or the water-soluble fraction of bio-oil) by hydroprocessing and zeolite upgrading to various products. The thermally unstable carbonyl functionalities in bio-oil go directly to coke on the zeolite catalyst, bypassing the desired commodity chemicals, including aromatic hydrocarbons, olefins, and alcohols. The carbonyl functionalities are converted to thermally stable corresponding alcohols upon hydrogenation, and the coke yield decreases in zeolite upgrading. A second hydrogenation step further increases the $H/C_{eff}$ ratio of feed, resulting in even lower coke yields in zeolite upgrading.

Figure S1 shows different process options we used in this study for the conversion of pyrolysis oil. The crude pyrolysis oil can be subjected directly to our process, or it can first be phase-separated into an aqueous and an organic phase by the addition of water. The organic phase of the bio-oil mainly contains high-molecular-weight lignin-derived phenolic oligomers (*23*). These lignin oligomers can be used to make phenol-formaldehyde resins (*24*) or as a low-cost feedstock for the base catalyzed depolymerization processes (*25*–*27*) to produce phenolic compounds or aromatic fuel (*28*–*30*). To exploit the advantages of hydroprocessing and zeolite upgrading for the upgrading of pyrolysis oil, we opted to study three different processing steps that can be operated in series: a low-temperature hydrogenation step using a Ru-based catalyst, a higher-temperature hydrogenation step using a Pt-based catalyst after the Ru-based step, and a zeolite conversion step. The Ru catalyst was chosen based on our previous experimental and theoretical studies on aqueous-phase acetic acid hydrogenation over monometallic catalysts (*31*). The conclusion from this study was that Ru was the most active and selective monometallic catalyst for aqueous-phase acetic acid hydrogenation at low temperatures. Pt was chosen as the catalyst for the high-temperature hydrogenation, because previous studies for hydrodeoxygenation of sorbitol have indicated that Pt catalysts have high C-O hydrogenation and low C-C bond cleavage activity (*32*). We explored these conversion options with two different pyrolysis oil feeds: crude bio-oil obtained from the U.S. Department of Energy's National Renewable Energy Laboratory (DOE-BO), and the water-soluble fraction of a pinewood bio-oil (WSBO). The WSBO sample was made by mixing pinewood bio-oil and water in a 1:4 weight ratio (*33*). For the DOE-BO sample, we compared the outcomes of zeolite upgrading with and without preceding low-temperature hydrogenation. For the WSBO sample, we examined these two protocols as well as the third, incorporating a high-temperature hydrogenation step between the low-temperature hydrogenation and zeolite upgrading steps.

Gas chromatography (GC) and high-peformance liquid chromatography (HPLC) of the DOE-BO (table S1) identified hydroxyacetaldehyde (9.0% of the total bio-oil carbon content), levoglucosan (8.8% of total bio-oil carbon), acetic acid (8.4% of total bio-oil carbon), sugars (1.8% of total bio-oil carbon), and hydroxyacetone (1.6% of total bio-oil carbon) as major components. Only one-third of the carbon content quantified by elemental analysis could be identified with these techniques. The remaining two-thirds of the carbon can be attributed to nonquantified compounds that are present in small quantities and GC- and HPLC-undetectable lignin and sugar oligomers. Gel per-

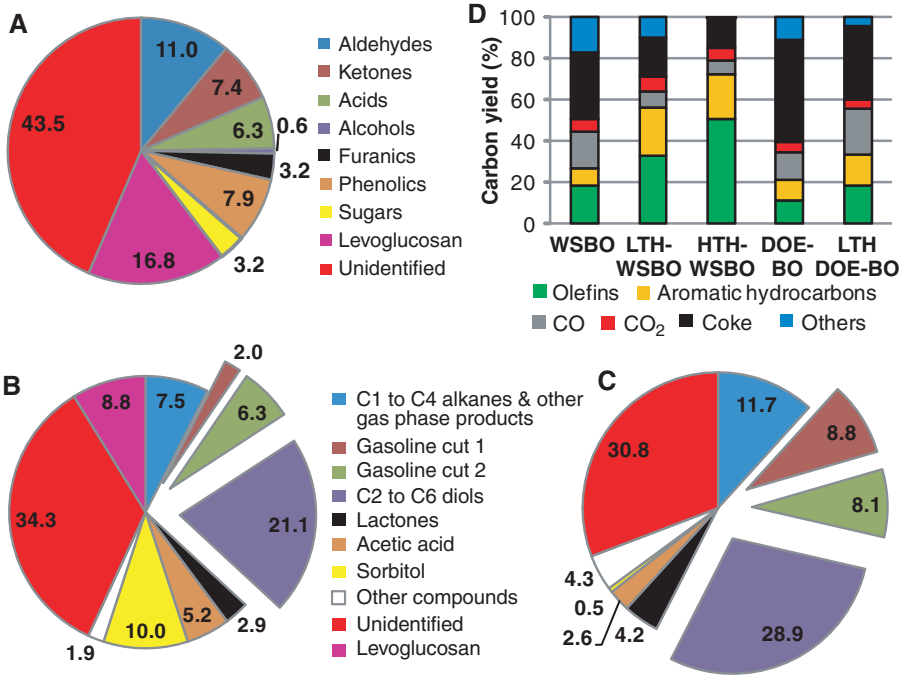


**Fig. 3.** Feed and product carbon distribution (in percent of carbon) for the hydrogenation of WSBO and for the zeolite upgrading. (**A**) WSBO feed. (**B**) Product distribution from single-stage hydrogenation of WSBO over Ru/C at 398 K and 52 bar at WHSV of 3 $hour^{-1}$. (**C**) Product distribution from two-stage hydrogenation of WSBO, first over Ru/C at 398 K and 100 bar at WHSV of 3 $hour^{-1}$, then over Pt/C at 523 K and 100 bar at WHSV of 3 $hour^{-1}$. (**D**) Carbon yields for the conversion of bio-oil–derived feedstocks over HZSM-5 at 873 K. WSBO. water-soluble fraction of the pinewood bio-oil; LTH-WSBO, WSBO hydrogenated over Ru/C (at 398 K and 52 bar at WHSV of 3 $hour^{-1}$); HTH-WSBO, WSBO hydrogenated first over Ru/C (at 398 K and 100 bar at WHSV of 3 $hour^{-1}$), then over Pt/C (at 523 K and 100 bar at WHSV of 3 $hour^{-1}$); DOE-BO. DOE bio-oil; LTH-DOE-BO, DOE bio-oil hydrogenated over Ru/C (at 398 K and 100 bar at WHSV of 1.6 $hour^{-1}$). The category "others" encompasses phenol, alkyl phenols, naphthol, and alkyl naphthols. The product groups defined in (B) and (C) contain the following components: C1 to C4 alkanes and other gas-phase compounds: methane, ethane, propane, butane, and other gas-phase compounds that have not been identified. Gasoline cut 1 (boiling range 338 to 373 K): pentane, hexane, methanol, ethanol, 1-propanol, tetrahydrofuran, 2-butanol, and 2-methyltetrahydrofuran. Gasoline cut 2 (boiling range 388 to 448 K): 1,2-cyclohexanediol, 2,5-dimethyltetrahydrofuran, 1-butanol, 2-pentanol, 1-pentanol, cyclopentanol, 2-hexanol, 3-methylcyclopentanol, cyclohexanol, 3-methylcyclohexanol, and 4-methylcyclohexanol. C2 to C6 diols: 2,3-butanediol, propylene glycol, ethylene glycol, 1,2-hexanediol, 1,4-hexanediol, 1,4-butanediol, and 1,4-pentanediol. Lactones: γ-butyrolactone and γ-valerolactone. Other compounds: tetrahydrofurfuryl alcohol, 1,2,6-hexanetriol, 1,2,3-butanetriol, and glycerol.

meation chromatography (GPC) (fig. S2) of DOE-BO confirmed the presence of oligomers ranging in molecular weight from 300 to 7000 daltons. Analysis of the WSBO by GC and HPLC identified the compounds composing 56.5% of the total carbon content (Fig. 3A and table S3). The most abundant functionalities in the WSBO included carbonyl compounds (24.7% of total WSBO carbon), carbohydrates (20% of total WSBO carbon; includes sugars and levoglucosan), and phenolics (7.9% of total WSBO carbon). The WSBO had an $H/C_{eff}$ ratio of 0.14. The unidentified carbon in the WSBO is most likely present as undetectable lignin and sugar oligomers.

We next examined the composition of the product stream from low-temperature hydrogenation of the DOE-BO. The $H/C_{eff}$ ratio rose from 0.06 to 0.09, with about 0.9 g of hydrogen consumed per 100 g of carbon in the feed during this step. The water content of the bio-oil also increased from 24.8 to 27 wt % during the low-temperature hydrogenation step. At the same time, the proportion of carbon content identifiable by GC and HPLC went down (table S2), perhaps as a result of homogeneous thermal polymerization reactions among the bio-oil components. The GPC analysis of the hydrogenated DOE bio-oil (fig. S2) shows higher concentrations of oligomers with molecular weights greater than 400 daltons as compared to the feed. The amount of thermal coke formed from DOE-BO was reduced from 19.0 to 13.6 wt % upon low-temperature hydrogenation (table S7). This implies that the product of low-temperature hydrogenation of DOE-BO is more thermally stable than the feed.

In the case of the water-soluble fraction of the WSBO, the $H/C_{eff}$ ratio increased from 0.14 to 0.71 after low-temperature hydrogenation and rose further to 1.20 upon high-temperature hydrogenation. Low-temperature hydrogenation was carried out at 398 K because it was found to be the lowest temperature at which all the pyrolysis oil functionalities started showing substantial activity toward hydrogenation. The compositions of the low-temperature hydrogenated WSBO and high-temperature hydrogenated WSBO, based on chromatographic analysis, are shown in Fig. 3 and in more detail in table S4. In the low-temperature hydrogenation, we were able to convert 29.4% of the WSBO feed carbon to gasoline cut 1, gasoline cut 2, and C2 to C6 diols (Fig. 3B), which can be marketed as products in their own right. Gasoline cut 1 comprises mainly small (up to three carbon atoms) monohydric alcohols that boil in the temperature range of 338 to 373 K. Gasoline cut 2 mainly contains C4 to C6 monohydric alcohols that boil in the temperature range of 388 to 448 K. The C2 to C6 diols boil above 450 K, with ethylene glycol and propylene glycol being the major components. These product groups can easily be separated by distillation. Gasoline cut 1 and gasoline cut 2 can be added to gasoline as renewable high-octane additives. Glycols can be further purified and sold. The thermal stability of the WSBO increases substantially after hydrogenation, with a homogeneous thermal coke yield decreasing from 12.8 wt % for the WSBO to 2.8 wt % for the WSBO after a low-temperature hydrogenation. The hydrogen consumption for the low-temperature hydrogenation process was 4.8 g of $H_2$/100 g of carbon in the feed.

However, the product distribution still contains substantial amounts of hydrogen-deficient compounds such as acetic acid ($H/C_{eff}$ ratio = 0), levoglucosan ($H/C_{eff}$ ratio = 0), and sorbitol

**Table 1.** Overall carbon yield for the integrated catalytic process for the conversion of pyrolysis oils and the aqueous fraction of pyrolysis oil. Carbon selectivity values are reported for the individual components benzene, toluene, xylene, ethylbenzene (EtBenz), ethylene, propylene, and butylene.

| Feed | Process | Hydrogen consumption (g/100 g of carbon in feed) | Final products (% carbon yield) or carbon selectivity (%) | | | | | |
|---|---|---|---|---|---|---|---|---|
| | | | C1 to C6 alkanes | $CO_x$ | Aromatics | Olefins | Coke | Unidentified |
| DOE-BO | Zeolite | None | 0 | 18.3 | 9.8 | 11.2 | 49.5 | 11.2 |
| | | | | | Carbon selectivity (%) | | | |
| | | | | | Benzene: 17.3 | Ethylene: 51.8 | | |
| | | | | | Toluene: 40.8 | Propylene: 36.6 | | |
| | | | | | Xylene: 23.5 | Butylene: 11.6 | | |
| | | | | | EtBenz: 2.0 | | | |
| DOE-BO | $Ru/H_2$ + Zeolite | 0.9 | 2 | 26.5 | 14.4 | 18.2 | 34.6 | 4.3 |
| | | | | | Carbon selectivity (%) | | | |
| | | | | | Benzene: 16.9 | Ethylene: 52.2 | | |
| | | | | | Toluene: 37.2 | Propylene: 35.9 | | |
| | | | | | Xylene: 38.5 | Butylene: 11.4 | | |
| | | | | | EtBenz: 3.4 | | | |
| WSBO | Zeolite | None | 0 | 23.7 | 8.2 | 18.5 | 32.3 | 17.3 |
| | | | | | Carbon selectivity (%) | | | |
| | | | | | Benzene: 26.8 | Ethylene: 41.6 | | |
| | | | | | Toluene: 46.3 | Propylene: 45.9 | | |
| | | | | | Xylene: 20.7 | Butylene: 12.4 | | |
| | | | | | EtBenz: 1.2 | | | |
| WSBO | $Ru/H_2$ + Zeolite | 4.8 | 7.5 | 13.9 | 21.6 | 30.2 | 17.4 | 9.4 |
| | | | | | Carbon selectivity (%) | | | |
| | | | | | Benzene: 17.6 | Ethylene: 31.8 | | |
| | | | | | Toluene: 45.5 | Propylene: 55.4 | | |
| | | | | | Xylene: 31.3 | Butylene: 12.8 | | |
| | | | | | EtBenz: 2.6 | | | |
| WSBO | $Ru/H_2$ + $Pt/H_2$ + Zeolite | 8.1 | 15.0 | 10.7 | 18.3 | 43.0 | 12.6 | 0.4 |
| | | | | | Carbon selectivity (%) | | | |
| | | | | | Benzene: 27.0 | Ethylene: 32.0 | | |
| | | | | | Toluene: 49.3 | Propylene: 53.8 | | |
| | | | | | Xylene: 19.1 | Butylene: 14.2 | | |
| | | | | | EtBenz: 2.3 | | | |

($H/C_{eff}$ ratio = 0.33). By feeding this stream through a high-temperature hydrogenation reactor at 523 K and 100 bar, the total carbon yield of gasoline cut 1, gasoline cut 2, and C2 to C6 diols increased to 45.8% (Fig. 3C and table S4). In this process, the product distribution can be customized by modifying the reaction conditions; for example, if there is a larger market for gasoline cut 1, its yield can be increased by operating the second stage at higher temperatures or lower space velocities. At higher temperatures, C2 to C6 diols undergo further C-O and C-C bond cleavage reactions, producing small monohydric alcohols. High-temperature hydrogenation was carried out at 23 K so as to achieve high sorbitol and levoglucosan conversion. In the high-temperature hydrogenation step, a 100% levoglucosan conversion and a 95% sorbitol conversion were obtained. An increase in carbon yield to the desired product groups of gasoline cut 1, gasoline cut 2, and C2 to C6 diols was observed, corresponding to the 80% of the levoglucosan and sorbitol carbon. Sorbitol can be converted over a supported Pt catalyst to a mixture of alcohols and polyols through reactions including hydrogenation, dehydration, decarbonylation, and retro-aldol condensation (*32*). Although sorbitol is substantially more thermally stable than glucose, it still has a low overall $H/C_{eff}$ ratio of 0.33 in comparison to the $H/C_{eff}$ ratios of the possible products from hydrogenolysis of sorbitol, including propylene glycol ($H/C_{eff}$ ratio = 1.33), propanol ($H/C_{eff}$ ratio = 2), and butanediols ($H/C_{eff}$ ratio = 1.5). The net hydrogen consumption for the combined low- and high-temperature hydrogenation process was 8.1 g of $H_2$/100 g of carbon in the feed. The WSBO had high thermal stability after the high-temperature hydrogenation, with the homogeneous thermal coke yield decreasing from 12.8 wt % for the WSBO to 0.2 wt % after high-temperature hydrogenation. High-pressure hydrogen is necessary in the high-temperature step to minimize carbon loss to less valuable C1 to C4 alkanes (*32*, *34*).

These hydrogenated feeds were then added to the zeolite step (step yields are in Fig. 3D and overall yields in Table 1). Only 20% of the DOE-BO carbon was converted to olefins and aromatics if fed directly to the zeolite without any hydrotreatment, with 50% of the carbon forming coke. The remaining 30% of the carbon was converted to CO, $CO_2$, and unidentified oxygenates. Low-temperature hydrogenation raises the yield of olefins and aromatics after zeolite upgrading to 32.6% (Table 1). The low-temperature hydrogenation step only used a small amount of hydrogen but resulted in a substantial increase in the yield of desired products. Similar results were observed with the water-soluble fraction of the WSBO. Direct zeolite upgrading of WSBO affords 26.7% carbon yield of olefins and aromatics. Low-temperature hydrogenation before zeolite upgrading raised the yield to 51.8%, whereas the high-temperature hydrogenation leads to 61.3% olefins and aromatics yield. The high-temperature hydrogenation process converts 15.0% of the carbon in WSBO to light alkanes, which is twice that of the low-temperature hydrogenation process. All these points are shown in Fig. 1 along with the theoretical yield, with toluene as the major product. The difference between experimental and theoretical yields is reduced with the increasing $H/C_{eff}$ ratio of the WSBO feed, indicating that the hydrogen added is used primarily for increasing the olefin and aromatics yield from the process. As seen in table S8, the percentage of theoretical toluene yield for the water-soluble fraction of the WSBO increased from 39.1 to 64.9% upon low-temperature hydrogenation and increased further to 72.3% upon high-temperature hydrogenation.

The major products obtained in the zeolite upgrading of DOE-BO and WSBO are C2 to C4 olefins and C6 to C8 aromatic hydrocarbons. Under the reaction conditions used in this study, the olefin selectivity for the DOE-BO and low-temperature hydrogenated DOE-BO was 52% to ethylene and 36% to propylene, with the balance being butylenes. The aromatic selectivity decreased with toluene (37 to 40% selectivity) > xylenes (23.5 to 38.5% selectivity) > benzene (17% selectivity). The olefin selectivity for the WSBO and hydrogenated WSBO was different than that of the DOE-BO, with an olefin selectivity of 45 to 55% to propylene and 32 to 42% to ethylene, with the balance being butylenes. The aromatic selectivity decreased with toluene (45 to 50% selectivity) > xylenes (20 to 30% selectivity) > benzene (17 to 27% selectivity). As we have demonstrated previously, the ratios of these products can be tuned by adjusting both the reaction conditions and catalytic process (*35*). For example, in the zeolite upgrading of high-temperature hydrogenated WSBO, the aromatic hydrocarbon–to–olefin ratio increases from 1:2.8 to 1:1.1 as the temperature is reduced from 923 to 673 K (table S6). Olefins can also be converted to aromatics by recycling the olefins back to the zeolite reactor. Several existing processes can also be used to convert olefins to aromatics, including olefin aromatization and alkylation of the aromatics using olefins (*36*, *37*). These results indicate that the olefin-to-aromatic ratio and the types of olefins and aromatics produced can be adjusted according to the market demand, using several approaches.

The cost of hydrogen is important in determining how much hydroprocessing should be done before deoxygenation with the zeolite catalyst. Figure 4 depicts the economic potential of our integrated catalytic process as a function of the $H/C_{eff}$ ratio of the feed-to-zeolite step for four different hydrogen costs. The economic potential of the process is calculated by subtracting the cost of process feeds (biomass and hydrogen) from the selling price of the products. Importantly, the economic potential includes only the costs of the raw material and does not include any other operating costs or capital costs. The market price of hydrogen varies widely depending on location, mode of supply, and natural gas prices. The cheapest hydrogen is from large steam reformers and typically costs $1.50 to $2.50/kg (*38*), whereas the hydrogen shipped in tube trailers can cost as much as $12/kg (*39*). The optimum $H/C_{eff}$ ratio, where the economic potential of the process is highest, decreases with increasing hydrogen cost. For example, if hydrogen cost is $2/kg, then the maximum economic potential occurs at an $H/C_{eff}$ of 1.4, whereas when the hydrogen cost is $4.20/kg, the maximum economic potential occurs when pyrolysis oil is fed directly to the zeolite catalyst without any hydrogenation. Combining the hydrogenation steps with a zeolite conversion step reduces the overall hydrogen requirements as compared to using hydrogen for a complete deoxygenation of pyrolysis oil. A complete deoxygenation of pyrolysis oil by hydrodeoxygenation, with a 100% carbon yield to the corresponding hydrocarbons

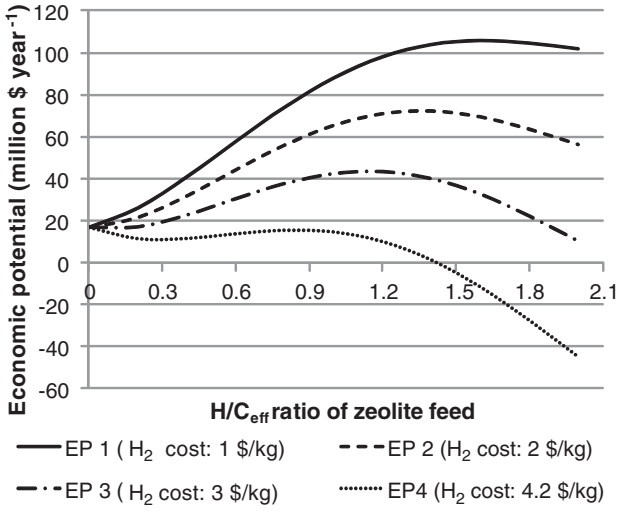


**Fig. 4.** Annual economic potential (EP) for the integrated hydroprocessing and zeolite upgrading of pyrolysis oil as a function of the $H/C_{eff}$ ratio of feed to zeolite catalyst. Data in Fig. 1 were used for calculating the economic potential values. The plant capacity was assumed to be 100 metric tons/hour of biomass. Pyrolysis oil yield was assumed to be 70 wt % of biomass. It was assumed that in the zeolite upgrading step, all olefins produced are converted to aromatics. A July 2010 spot price of benzene of $2.60/gallon was used as the aromatic hydrocarbon selling price (*43*). Biomass cost was assumed to be $50/ton.

(that is, alkanes from C1 to C6 nonphenolic oxygenates and aromatics from phenolic compounds), requires 14 to 15 g of $H_2$/100 g of carbon in the feed, if the catalyst coking problems are overcome. In comparison, increasing the $H/C_{eff}$ ratio of pyrolysis oil from 0 to 1.4 requires 11.7 g of $H_2$/100 g of carbon in the feed, reducing the hydrogen requirements as compared to complete hydrodeoxygenation by 20%. Furthermore, during the hydrotreating process, large amounts of undesired methane are produced, which also can substantially increase the hydrogen requirements. Hydrogen required in these processes should preferably be obtained from renewable sources, such as by the reforming of biomass-derived feedstock (*14*, *40*, *41*). Alternatively, hydrogen can be obtained from coal gasification or from water splitting driven by carbon-free energy sources, such as solar, nuclear, and wind energy, as suggested by Agrawal *et al.* (*42*). Zeolite catalysts convert the biomass feedstocks into aromatics and olefins, which can fit easily into the existing infrastructure. Increasing the yield of petrochemical products from biomass therefore requires hydrogen. Thus, there exists an optimum solution for the economical maximum yield of petrochemical feedstocks products that is dictated by the cost of hydrogen. It is expected that future advances in the field of metal and zeolite catalysts, combined with reaction engineering, will allow us to design even more efficient and economical processes to convert biomass resources to renewable chemical industry feedstocks.

### References and Notes


1. A. J. Ragauskas *et al.*, *Science* **311**, 484 (2006).
2. G. W. Huber, S. Iborra, A. Corma, *Chem. Rev.* **106**, 4044 (2006).
3. E. L. Kunkes *et al.*, *Science* **322**, 417 (2008).
4. D. L. Klass, *Biomass for Renewable Energy, Fuels and Chemicals* (Academic Press, San Diego, CA, 1998).
5. S. Czernik, A. V. Bridgwater, *Energy Fuels* **18**, 590 (2004).
6. D. Mohan, C. U. Pittman, P. H. Steele, *Energy Fuels* **20**, 848 (2006).
7. M. M. Wright, D. E. Daugaard, J. A. Satrio, R. C. Brown, *Fuel* 10.1016/j.fuel.2010.07.029.
8. R. P. Anex *et al.*, *Div. Fuel Chem.* **54**, 704 (2009).
9. A. Oasmaa, S. Czernik, *Energy Fuels* **13**, 914 (1999).
10. D. C. Elliott, *Energy Fuels* **21**, 1792 (2007).
11. T. L. Marker *et al.*, *Opportunities for Biorenewables in Petroleum Refineries* (Final Report, DE-FG36-05GO15085, UOP, Des Plaines, IL, 2005); www.osti.gov/bridge/servlets/purl/861458-Wv5uum/861458.pdf.
12. J. D. Adjaye, N. N. Bakhshi, *Fuel Proc. Tech.* **45**, 161 (1995).
13. J. D. Adjaye, N. N. Bakhshi, *Fuel Proc. Tech.* **45**, 185 (1995).
14. T. P. Vispute, G. W. Huber, *Green Chem.* **11**, 1433 (2009).
15. C. H. Bartholomew, R. J. Farrauto, *Fundamentals of Industrial Catalytic Processes* (Wiley, Hoboken, NJ, 2006).
16. T. F. Degnan Jr., M. Smith, C. R. Venkat, *Appl. Catal. A* **221**, 283 (2001).
17. C. Perego, P. Ingallina, *Catal. Today* **73**, 3 (2002).
18. G. R. Lappin, J. D. Sauer, Eds., *Alpha Olefins Applications Handbook* (Marcel Dekker, New York, NY, 1989).
19. H. H. Szmant, *Organic Building Blocks of the Chemical Industry* (Wiley, New York, 1989).
20. N. Y. Chen, T. F. Degnan Jr., L. R. Koenig, *Chemtech* **16**, 506 (1986).
21. A. G. Gayubo, A. T. Aguayo, A. Atutxa, R. Aguado, J. Bilbao, *Ind. Eng. Chem. Res.* **43**, 2610 (2004).
22. T. R. Carlson, T. P. Vispute, G. W. Huber, *ChemSusChem* **1**, 397 (2008).
23. R. Bayerbach, D. Meier, *J. Anal. Appl. Pyrolysis* **85**, 98 (2009).
24. T. A. Milne, F. Agblevor, M. Davis, S. Deutch, D. Johnson, in *Developments in Thermal Biomass Conversion*, A. V. Bridgwater, D. G. B. Boocock, Eds. (Blackie Academic and Professional, London, 1997), pp. 409–424.
25. J. S. Shabtai, W. W. Zmierczak, E. Chornet, U.S. Patent 5,959,167 (1999).
26. J. S. Shabtai, W. W. Zmierczak, E. Chornet, U.S. Patent 6,172,272 (2001).
27. J. E. Miller, L. Evans, A. Littlewolf, D. E. Trudell, *Fuel* **78**, 1363 (1999).
28. C. Zhao, Y. Kou, A. A. Lemonidou, X. B. Li, J. A. Lercher, *Angew. Chem. Int. Ed.* **48**, 3987 (2009).
29. S. Crossley, J. Faria, M. Shen, D. E. Resasco, *Science* **327**, 68 (2010).
30. C. Zhao, Y. Kou, A. A. Lemonidou, X. B. Li, J. A. Lercher, *Chem. Commun.* **46**, 412 (2010).
31. H. Olcay, L. Xu, Y. Xu, G. W. Huber, *ChemCatChem* 10.1002/cctc.201000134 (2010).
32. N. Li, G. W. Huber, *J. Catal.* **270**, 48 (2010).
33. Materials, methods, and calculations are available as supporting material on *Science* Online.
34. G. W. Huber, R. D. Cortright, J. A. Dumesic, *Angew. Chem. Int. Ed.* **43**, 1549 (2004).
35. T. R. Carlson, Y. Cheng, J. Jae, G. W. Huber, *Energy Environ. Sci.* 10.1039/C0EE00341G.
36. M. Guisnet, N. S. Gnep, F. Alario, *Appl. Catal. A* **89**, 1 (1992).
37. V. R. Choudhary, P. Devadas, S. Banerjee, A. K. Kinage, *Microporous Mesoporous Mater.* **47**, 253 (2001).
38. C. E. G. Padro, V. Putsche, *Survey of the Economics of Hydrogen Technologies* (report, NREL/TP-570-27079, National Renewable Energy Laboratory, Golden, CO, 1999); http://www1.eere.energy.gov/hydrogenandfuelcells//pdfs/27079.pdf.
39. National Research Council and National Academy of Engineering, *The Hydrogen Economy: Opportunities, Costs, Barriers, and R&D Needs* (National Academies Press, Washington, DC, 2004).
40. R. D. Cortright, R. R. Davda, J. A. Dumesic, *Nature* **418**, 964 (2002).
41. G. W. Huber, J. W. Shabaker, J. A. Dumesic, *Science* **300**, 2075 (2003).
42. R. Agrawal, N. R. Singh, F. H. Ribeiro, W. N. Delgass, *Proc. Natl. Acad. Sci. U.S.A.* **104**, 4828 (2007).
43. ICIS pricing report, www.icis.com/v2/chemicals/9075158/benzene/pricing.html.


44. This work was supported by the U.S. Department of Energy Office of Energy Efficiency and Renewable Energy, under grant DE-FG36-08GO18212; and by the Defense Advanced Research Projects Agency (DARPA) through the Defense Science Office Agreement HR0011-09-C-0075) (Approved for Public Release, Distribution Unlimited); the National Basic Research Program of China (973 Program, grant no. 2010CB732206); and the National Natural Science Foundation of China (grant no. 51076031). The views, opinions, and/or findings contained in this article/presentation are those of the author/presenter and should not be interpreted as representing the official views or policies, either expressed or implied, of the DARPA or the Department of Defense. We thank A. Javaid for the microfiltration of bio-oil, Y. Cheng for help with zeolite upgrading experiments, and the National Renewable Energy Laboratory and P. H. Steele from the Forest Products Department at Mississippi State University for providing us with bio-oil samples. The University of Massachusetts has filed a patent based on the methods presented here. G.W.H. has a financial interest in Anellotech, a privately held company focused on producing renewable petrochemicals from biomass.


### Supporting Online Material

www.sciencemag.org/cgi/content/full/330/6008/1222/DC1
Materials and Methods
Figs. S1 and S2
Tables S1 to S8

24 June 2010; accepted 13 October 2010
10.1126/science.1194218

# The Core Structure of Basal Dislocations in Deformed Sapphire ($\alpha$-$Al_2O_3$)

**A. H. Heuer,[1]*† C. L. Jia,[2]* K. P. D. Lagerlöf[1]**

**The atomic structure of dislocation cores is decisive for the understanding of plasticity in crystalline solids. The core structure of dislocations in sapphire introduced by high-temperature plastic deformation has been investigated with the use of the negative spherical-aberration imaging technique. The ability of this technique to discriminate oxygen columns from aluminum (Al) columns, combined with reproduction of subtle contrast features by image simulation, leads to a markedly detailed atomic model of the dislocation cores. The partial dislocations are Al-terminated, with electrical neutrality being achieved because half of the Al columns are missing. These partials also undergo core spreading, which results in random occupancy of both tetrahedrally and octahedrally coordinated sites, though Al in tetrahedral coordination never occurs in a perfect crystal. Unusual dislocation core structures may be present in other technologically important nonmetallic solids.**

Although ceramics are notorious for their brittle behavior under normal service conditions, plastic deformation in such materials can be realized at elevated temperatures, under circumstances in which friction and wear occur, and wherever cracking is suppressed by confining pressures, such as under an indentation. Under all of these conditions, the behavior of dislocations, the principal "carrier" of plastic deformation in crystalline materials, assumes paramount importance.

Aluminum oxide ($\alpha$-$Al_2O_3$) in both single-crystal form (sapphire) and as dense polycrystals finds utility in a wide range of important